Massive Access for Machine-to-Machine Communication in Cellular Networks

Massive Machine-to-Machine Communication in Long Term Evolution and Long Range Wide Area Network

Project Report

Group 1052

Aalborg University
Electronics and IT

Here you can write something about which tools and software you have used for typesetting the document, running simulations and creating figures. If you do not know what to write, either leave this page blank or have a look at the colophon in some of your books.

AALBORG UNIVERSITY
STUDENT REPORT

Electronics and IT
Aalborg University
http://www.aau.dk

Title:
Massive Access for Machine-to-Machine Communication in Cellular Networks

Theme:
Master Thesis

Project Period:
Spring & Fall Semesters 2015/2016

Project Group:
1052

Participant(s):
René Brandborg Sørensen

Supervisor(s):
Dong Min Kim
Petar Popovski

Copies: 1

Page Numbers: 54

Date of Completion:
June 1, 2016

Abstract:

In this report a traffic model for massive low-rate machine-to-machine communications is presented and used in an evaluation of LTE-MTC and LoRaWAN.
Outage and latency for both LTE-MTC and LoRaWAN are obtained through simulation and a tractable model for LoRaWAN is found through analysis. A transmission scheme in which transmissions occur in parallel by LTE-MTC and LoRAWAN is also analysed as is a scheme in which LoRaWAN is used to form capillary networks within an LTE-MTC cell.
LTE-MTC is found to provide a high capacity, low latency network capable of handling a high device density while LoRaWAN is found to provide a lower capacity, in general higher latencies and accommodate only low device densities. A trade-off must be made between cost and QoS requirements at the device-side to chose technology.

Contents

Preface

This thesis is made as a completion of the master programme in Wireless Communication Systems. Yours truly has a bachelor degree in Electronics and IT from Aalborg University and this thesis is the product of the last two semesters at the Wireless Communication Systems study at Aalborg University.

I would like to thank my supervisors Petar Popovski and Dong Min Kim for their valuable support and feedback throughout the project period. Furthermore I would like to thank Germán Corrales Madueño whose support and guidance I enjoyed through the first semester of my master thesis, through several projects on the bachelor and on the master programme where I also enjoyed the supportive supervision of Nuno Kiilerich Pratas. I have immensely enjoyed my student job at the M2M group and I am very thankful for the tutoring I have experienced through my studies and in my student job.

The Matlab-based simulators for LTE-MTC, LoRaWAN and the capillary scheme may be found at `https://github.com/RBS92/thesis`.

Aalborg University, June 1, 2016

René Brandborg Sørensen
<rsaren11@student.aau.dk>

Chapter 1

Introduction

This chapter contains an introduction of massive machine-to-machine (M2M) communication and presents the state of the art within this field in short. Lastly a scenario considering M2M communication in a Radio Access Network (RAN) is defined and a research problem is formulated.

1.1 Massive Machine-To-Machine Communications

In the next decade a massive increase in the global cellular traffic volume is expected. Predictions vary from a factor 70 increase in cellular traffic in 2020 compared to 2010, to a factor 1000 increase in wireless-traffic [1]. Services provided by machines in our society is going to rapidly expand with services such as health monitoring, security monitoring and smart grid services. The services provided by machines in the Internet of Things (IoT) and "big data" will not only incite large societal changes, but they also generate new demands for wireless networks, which are expected to provide internet access for most of these machines.

M2M communication is defined as the communication between autonomous devices. Such a device is known in 3GPP terminology as machine type device (MTD). M2M communication covers a large variety of use-cases, which are examined in the next chapter. Equipment where radio link failure could be life-threatening will require an enormous reliability and devices, for which timing is critical, the packet may need to be delivered almost instantly after being generated. Some M2M services require high data rates for a few devices, e.g. remote backup of a security camera feed, which resembles human originating traffic (H2*), while for example massive sensory systems require a relatively low data rates for a massive number of devices.

The problem of massive access in wireless networks is introduced by the latter case. The wireless networks of today are developed with the aim of supporting H2* traffic, which is characterized by bursty traffic for a relatively small number of users with high data demands. 50 billion connected MTDs have been predicted by 2020 [1]. An increase of 45 billion devices compared to the 5 billion connected devices in 2010. This predicted demand for wireless M2M services has incited massive research and development of cellular and capillary technologies for supporting the disperse M2M traffic.

Among the factors to be considered regarding machines in the IoT is the price of the cellular transceivers and the lifetime of the devices. GSM is currently the main cellular technology used for M2M applications. 64% of M2M devices are connected by GSM-only while 25% is connected by HSPA and 1% is connected by LTE while the last 10% is connected by WCDMA[2]. GSM is an inexpensive solution compared to UMTS and LTE, but it is less spectrally efficient and it is expected that operators will re-harvest the spectrum for LTE or 5G services. This poses a problem considering that the lifetime of many M2M devices is several years. Power efficiency must also be considered as many devices are expected to be powered by a single embedded battery for the devices entire lifetime.

1.1.1 State of the art

Initial research into determining M2M scenarios and characterising the associated traffic parameters has been done and 3GPP has characterized M2M-scenarios, -traffic and requirements in [3] and [4].

The M2M capacity of current RANs has been investigated in [5, 6, 7, 8]. GSM has been investigated in [5] and found to achieve a considerable capacity for M2M traffic with relatively few adjustments to prevent bottlenecking. Random Access in LTE is shown to bottleneck M2M traffic in [6, 7]. In [6] it is shown how LTE supports a large number of smart meters reporting periodically, but traffic expected in future smart meters, will have a large impact on the quality of service (QoS). A QoS model of LTE considering the random access procedure and transmission is contributed by [7] and further developed in [8] to include resource starvation in both control and transmission channels. This research shows that current RANs may be able to handle some M2M traffic, but they are not geared to handle the M2M traffic of the future.

Improvements of the RANs capabilities to handle M2M traffic has been investigated in [9] and [10]. Congestion control for RANs with M2M traffic is especially of interest, as the RANs were originally designed for H2* traffic and the M2M traffic may be regarded as an interference. IEEE 802.11p is an amendment to the IEEE Standard "Air Interface for Broadband Wireless Access Systems". The amendment is entitled "Enhancements to Support Machine-to-Machine Applications" and offers lower power consumption at devices and support for a significantly larger amount of users at the base station (BS).

Protocols for M2M communications are under development. Some offer "clean slate" utilization of spectrum, some are compatible with legacy systems and some are intended for use in unlicensed spectrum. The generators of these protocols are mainly IEEE, 3GPP and proprietors in the industry.

Cellular protocols such as extended coverage GSM (EC-GSM) and LTE-MTC (LTE-M) provide excellent coverage and data rates, but are costly compared to proprietary solutions like Sigfox and LoRa, which both aim to deliver excellent coverage, but at different data rates. The new IEEE 802.11ah protocol is WiFi-based and promises the ability to handle a large number of stations at each access point and provide up to 1 km radius of coverage. Weightless is the name of a set of Low-Power Wide-Area Network (LPWAN) open standards for M2M communications. Weightless-N uses Ultra Narrow Band (UNB) for transmission and operates in the Industrial, Scientific, and Medical (ISM) band like Sigfox. Weightless-W operates in white spaces within the terrestrial television broadcast band. These protocols, which are being developed for M2M, are listed in Table 1.1 and Table 1.2.

Protocol	Sigfox	Lora	Weightless-N	Weightless-W	802.11ah
Association	Proprietary	Proprietary	Open standard	Open standard	IEEE
Spectrum	Unlicensed	Unlicensed	Unlicensed	White space	Unlicensed
Band	ISM (UNB)	ISM	ISM (UNB)	White space	ISM
Cost	Low	Low	-	-	-
ETA	Availible	Availible	-	-	2016

Table 1.1: Protocols for capilary networks being developed for M2M communication scenarios

Protocol	EC-GSM	LTE-M	NB LTE-M	NB IoT
Association	3GPP	3GPP	3GPP	3GPP
Spectrum	Licensed	Licensed	Licensed	Licensed
Band	GSM	LTE	LTE & GSM	LTE & GSM
Cost	Low	Low-Medium	Low	-
ETA	2016	2016	2016	2016

Table 1.2: Protocols for cellular networks being developed for M2M communication scenarios

EC-GSM, LTE-M and NB LTE-M will not be available before 2016 while 5G is envisioned to be finished beyond 2020. The propitiatory networks, LoRa and Sigfox, are however available today. Other access networks exist, which may serve M2M devices in specific scenarios. Such as power line communication (PLC) and and satellite communication.

1.2 Problem statement

In this section a problem to be examined throughout this project is formulated.

1.2.1 Problem definition

Figure 1.1 shows a scenario in which a group of M2M devices wish to communicate with an M2M server located on the internet. The M2M devices are connected to the internet through a cellular connection, such that the M2M traffic passs through the RAN to the core network before being sent through the internet towards the targeted M2M server.

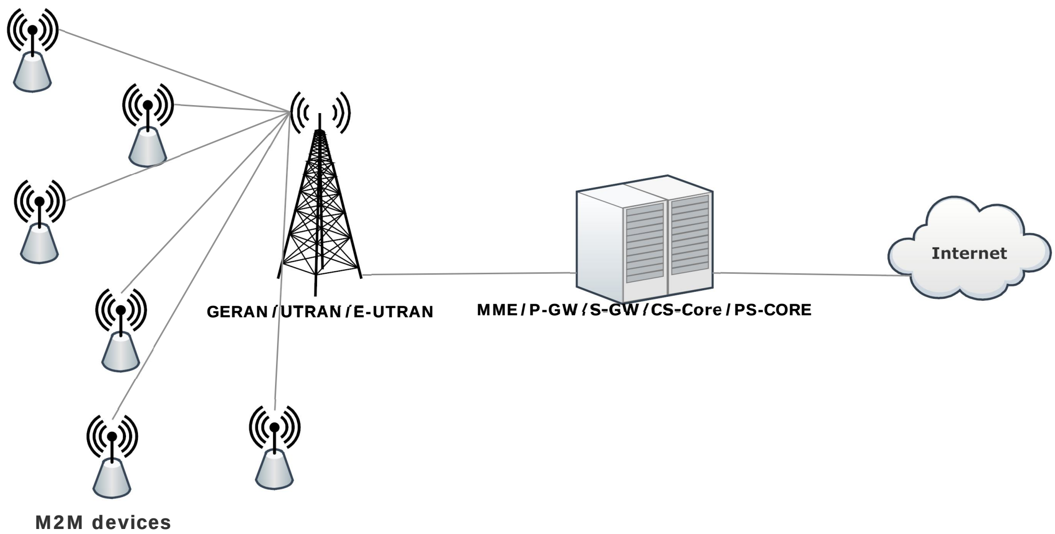

Figure 1.1: Scenario overview: MTDs, RAN and Backbone

M2M traffic differs from H2* traffic as previously noted. In particular a characteristic M2M scenario is to have a massive number of devices transmitting small payloads as opposed to having a small number of UEs transmit large packets. The same amount of data is transmitted when 10000 devices transmit 100 bytes of data, as when 100 devices transmit 10000 bytes of data. The overhead and bottleneck in the two cases is, however, not the same. Throughout the protocol stacks, from the M2M application to the M2M server, layers of signalling overhead is added to any transmitted data. This introduces bottlenecks in both RANs and backbone networks. These bottlenecks must be identified within the next decade to accommodate and allow the explosive growth in the number of M2M devices.

In [3] annex A three cases are defined for the network infrastructure.

- Radio Network Congestion case
- Core Network Congestion case

- Signalling Network Congestion case

This project will be focused on the Radio Network Congestion case. Cellular protocols and capillary protocols intended for M2M traffic are under development as previously noted. This project aims to extend the state of the art by evaluating the performance new cellular and capillary protocols with regards to massive M2M and assessing the role of these new protocols in future M2M deployments.LTE-M has been chosen as an interesting candidate for this investigation as it is deployable in current LTE networks by a software update at the BS and is expected to be a reliable and high throughput cellular connection at a lower cost than LTE for cellphones. LoRa is an interesting capillary candidate as it brings a robust modulation scheme and long range at a low cost for M2M devices.

In order to provide this investigation several topics need clarification.

1. Characterization of M2M scenarios and associated traffic and environment metrics
   (a) M2M service requirements
   (b) Specification of traffic parameters
   (c) Temporal and spatial traffic model
   (d) Environmental model
2. LTE-MTC
   (a) Investigate LTE-MTC protocol
   (b) Build Simulator and/or Model LTE-M
   (c) Evaluate performance of direct LTE
3. Long Range
   (a) Investigate LoRa protocol
   (b) Build Simulator for and/or Model LoRa
   (c) Evaluate performance
4. Evaluate performance of scenarios with
   (a) LTE-M only enabled devices
   (b) LoRa only enabled devices
   (c) LTE-A and LoRa enabled devices

Chapter 2

Machine-to-machine

In this chapter a traffic model for M2M is presented. The purpose of the traffic model is to characterize the M2M traffic and define requirements for M2M type traffic.

2.1 Traffic and environmental characteristics

In this section M2M scenarios are examined and the characteristics of M2M traffic is examined. The purpose is to model the traffic such that this may be used to evaluate the impact of M2M traffic in RANs.

2.1.1 Use cases and service requirements

M2M communications covers a large number of use-cases. The service requirements can range from connectivity of massive number of devices to ultra-reliable and real-time communications to high throughput. Current cellular is designed for the latter case as this is the primary service demand for H2* traffic. Service scenarios for the next generation (5G) may be found in [11] and cover among others:

- "Ubiquitous things communicating" focusing on handling a large number of devices.
- "Super real-time and reliable connections" focusing on new use cases with very low latency and high reliability requirements.

"Ubiquitous things communicating" is a service scenario intended for massive numbers of M2M devices that are expected. The devices may range in complexity and QoS requirements from low-rate sensors and actuators to more complex eHealth devices.

Table 2.1: Cell parameters

Parameter	Cell radius	Cell area	Household density	Households	Device density	Devices
Value	577.3 m	0.86 km^2 (assuming hexagon)	1517 km^{-2}	1304	60680 km^{-2}	52185

Table 2.2: Channel characteristics

Parameter	Path loss	Shadowing variance	Multipath (Rayleigh) scale parameter
Value	FRIIS	3	0.5

"Super real-time and reliable connections" is intended for machines with tasks requiring a highly reliable and low latency transmission interface, such as devices in the power distribution grid and devices ensuring traffic safety.

2.1.2 Environmental characteristics

IoT covers a wide array of use-cases in varying environments. The device density and composition changes with the environment as do the characteristics of the wireless medium. This leads to differences in traffic characteristics and link quality between different environments. It is expected that the highest device density will be found in an urban environment. The urban environment may then be considered to be a worst case scenario for a cellular network, which provides a "Ubiquitous things communicating"-service.

Consider an urban scenario equivalent to that considered in [12]. The cell parameters are given in Table 2.1. A hexagon cell is assumed for calculation of the cell area and number of devices and clusters within the cell. Such that these numbers resemble what would be found in an actual deployment. The cell is, however, for all other purposes assumed to be perfectly round to simplify the positioning of devices.

Two placement options of devices will be considered: A uniform distribution of devices and a uniform distribution of clusters of devices.

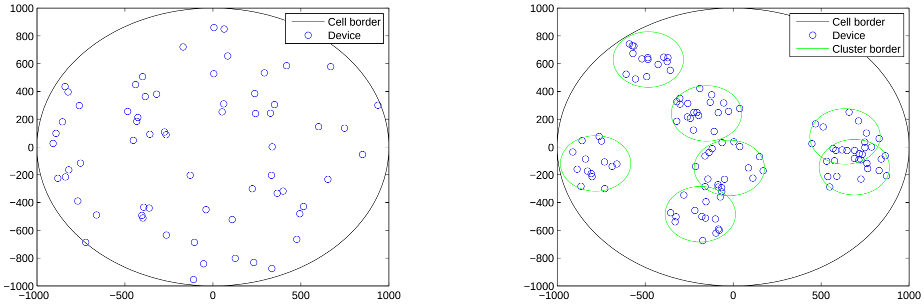

(a) Uniform **(b)** Clusters

Figure 2.1: Random positioning options

2.1.3 Traffic characteristics

3GPP has defined an aggregated arrival model for low-complexity M2M devices in [4] and in annex E of [12] four traffic types are defined. These traffic models have been assimilated to create a source traffic model.

- Mobile Autonomous reporting (MAR) exception reports
- Mobile Autonomous reporting (MAR) periodic reports
- Network Command
- Software update/reconfiguration

Table 2.3 shows the traffic characteristics of the four types of traffic.

MAR exception reports

MAR exception reports are sent by devices which are triggered by an event. This type of reports could for instance be generated by sensors such as smoke alarms, earthquake sensors or power outage notifications. It is assumed the event has epicentre within the cell and that the event triggers an event wave, which propagates through the cell at a given speed. In [13] it is shown that this model results in alarm reports, which are beta distributed in time. The parameters of the Beta distribution are dependent on the location of the event-epicentre and the event-wave propagation speed. In Figure 2.2 a cell radius of 1000 m is considered, an event-epicentre has been chosen to be 500 m (halfway) from the cell edge and the event-wave speed has been chosen to be 150 m/s, which results in a period of the distribution of 10 s.

In this way beta distributions can be generated, which have a period of 10 s as the beta distribution proposed by 3GPP in [4], but the parameters of the beta

Table 2.3: 3GPP traffic model for low-complexity M2M devices as per [4]

Type	Payload	Inter-arrival time	Maximum latency	Up-/Downlink
MAR exception	20 bytes	Arrivals are Beta distributed in time	10 s	Uplink
MAR periodic	Paretto distributed, alpha = 2.5, starting at 20 bytes with cut-off at 200 bytes.	Devices are split into groups of exponential inter-arrival times: 1 day for 40%, 2 hours for 40%, 1 hour for 15% and 30 minutes for 5%.	-	Uplink
Network Command	20 bytes	Same as for MAR periodic	-	Downlink / 50% triggers uplink response with a payload modeled as for MAR periodic.
Software update & reconfiguration	Peretto distributed, alpha=1.5, starting at 200 bytes with cut-off at 2000 bytes.	Exponential inter-arrival time of 180 days	-	Downlink

distribution are inherited from the event-wave model. This will allow for the implementation of different events when an event-propagation speed can be found.

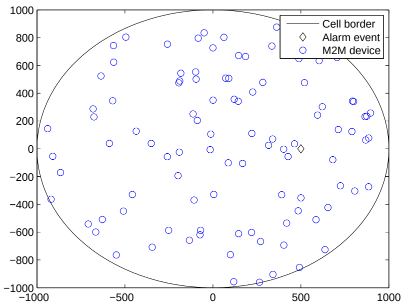

(a) T = 0

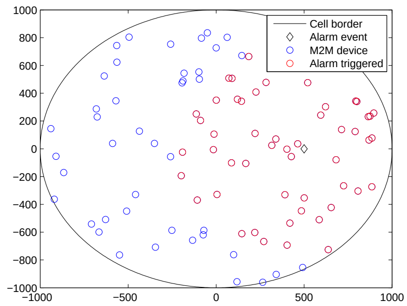

(b) T = 5 s

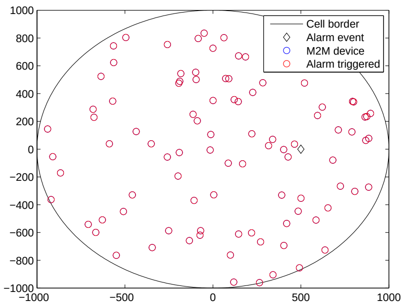

(c) T = 10 s

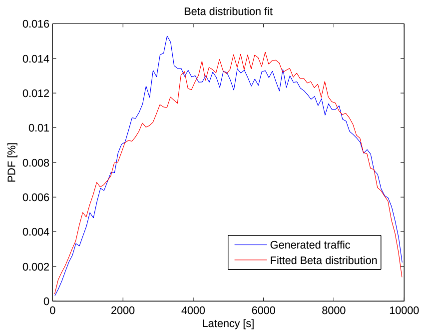

(d) Beta fit

Figure 2.2: Event triggering by event wave model and comparison to fitted Beta distribution

The reports are required to be delivered in near real-time at 10 s.

MAR periodic reports

MAR periodic reports are sent in the uplink and expected to be common in many IoT use cases. These reports are assumed to have a payload which is Pareto distributed with shape parameter, alpha, equal to 2.5, the minimum application payload size being 20 bytes and a cut-off at 200 bytes. In [12] generated payloads beyond the 200 bytes are set to 200 bytes. This leads to a very scewed distribution, which is avoided in this model by adjusting the Pareto pdf such that it is 0 beyond 200 bytes. The inter-arrival time of this type of traffic is split into 1 day for 40%, 2 hours for 40%, 1 hour for 15% and 30 minutes for 5%. A downlink application layer ACK is assumed to be sent for 50% of the MAR periodic reports.

Protocol Header	Overhead (size)
CoAP	4 bytes
DTLS	13 bytes
UDP	8 bytes
IP	40 bytes (4 bytes compressed)
In Total	65 bytes (29 bytes compressed)

Table 2.4: Protocol header sizes

Network Command traffic

Network Command traffic is generated by application servers. The network command traffic consists of application layer commands. It is assumed that 50% of network commands in the downlink will trigger an uplink response. No acknowledgement is sent for the uplink response. The payload size of this kind of traffic is assumed to be 20 bytes and the inter-arrival time is assumed to be the same as for the MAR periodic reports. The payload size of the uplink response is modelled equivalent to the payload size for the MAR periodic reports.

Software update/reconfiguration

Software update/reconfiguration are expected to occur periodically. Software reconfiguration is expected to make up most of these events. The application payload size is assumed to be Pareto distributed with parameter alpha equal to 1.5, a minimum size of 200 bytes and a cut of at 2000 bytes. The inter-arrival time is 180 days.

2.1.4 Protocol overhead

The total header size is equivalent to the sum of the header overhead in each layer. Let's consider the protocol stack of Table 2.4.

The Datagram Transport Layer Security (DTLS) protocol provides communications privacy for datagram protocols. It is designed to prevent eavesdropping, tampering, and message forgery. The DTLS header size may be quite large, but it may be sent as more fragments. A size of 13 bytes is chosen for the header as in [12]. Constrained Application Protocol (CoAP) uses a binary header of 4 bytes to provide a request/response between application endpoints over UDP. User Datagram Protocol (UDP) provides a procedure for applications to send messages to other applications. Delivery and duplicate protections is not guaranteed in UDP. CoAP, however, allows for a level of reliability for applications that need it. The UDP header size is 8 bytes. UDP assumes that the Internet Protocol (IP) is used as the underlying protocol. The IP header is assumed to be 40 bytes, but can be compressed down to a size of 4 bytes.

2.2 Delimitation of traffic model

Downlink initiated traffic may be transmitted to specific devices or broadcast. Paging may be carried out for single devices or device groups. This presents a research opportunity to find the best method for addressing and allocating resources in the downlink for M2M. This will, however, require models of the device and service composition of M2M within a given cell. In this work only uplink initiated traffic will be considered. The MAR exception and MAR periodic traffic of Table 2.3 fit this requirement.

Chapter 3

Long Term Evolution

The Evolved Packet System (EPS) consists of several domains. Each domain consists of a group of nodes and provides a set of features for the network. One type of domain within EPS is the RAN domain. Different RAN domains exist for 2G, 3G, LTE and secular non-3GPP protocol domains. The domains are distinguished to allow for the EPS to handle the signalling and security appropriately for users within each domain. The RAN domains handle radio-related features for EPS including scheduling, radio-resource handling, retransmission, coding and various multi-antenna schemes. The core network consists of multiple domains - the Circuit Core, Packet Core, IP Multimedia Subsystem (IMS) and the subscriber data management as depicted in Figure 3.2. The network core domains provide access to Circuit Switched (CS) networks and IP networks on the periphery of the EPS system.

LTE/LTE-A is the 4th generation of RAN. It was developed in parallel to the work in SAE to develop the evolved packet core (EPC). LTE and EPC are packet oriented systems contrary to circuit oriented. This change was prompted by a growing mobile broadband market. Hence LTE and EPC were designed to deliver high bandwidth and low latency for mobile broadband users. This chapter will provide insight into LTE.

3.1 LTE/LTE-A

Long Term Evolution (LTE) is the fourth generation of cellular radio access networks in 3GPP. LTE release 10 was given the name LTE-Advanced (LTE-A) for the purpose of International Telecommunication Union (ITU) submission. ITU-R determined two candidates for International Mobile Telecommunications-Advanced (IMT-Advanced) being LTE-A and WirelessMAN-Advanced in October 2010. A large motivator for the 4G evolution was mobile broadband and hence LTE moved to IP-based services, for example, LTE handles voice calls by voice over IP (VoIP)

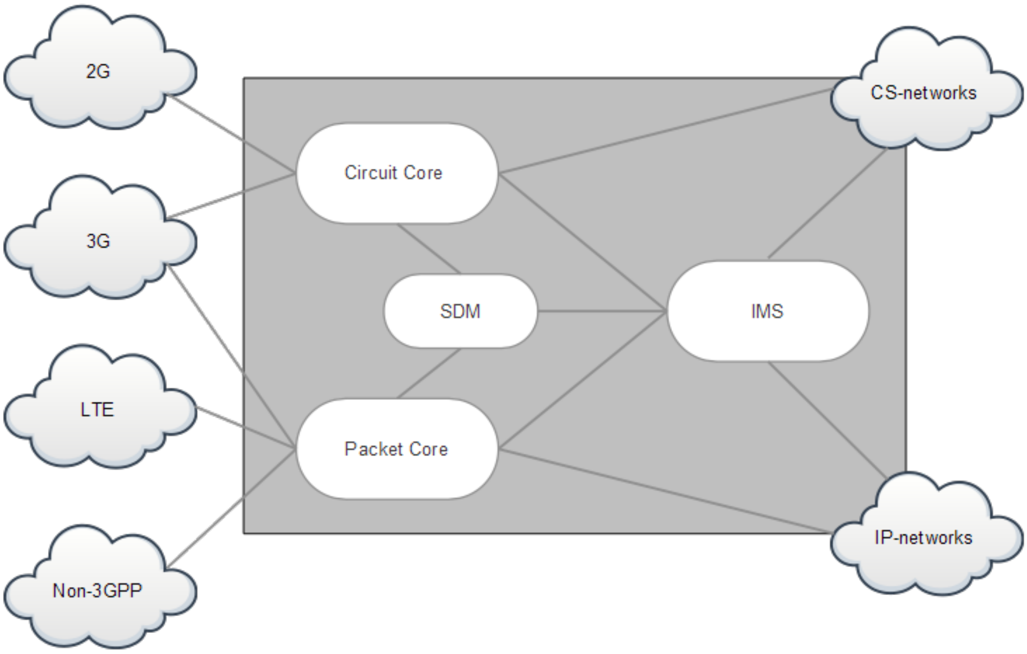

Figure 3.1: EPS domain architecture [14]

contrary to circuit switching in GSM. LTE was furthermore designed to provide high data rates and to ensure QoS for the IP traffic. The spectral efficiency - the ratio of data rate to bandwidth - is higher in LTE than in the prior cellular standards namely 2G and 3G systems and the latency is low <5 ms for small IP packets in good conditions [15].

Work continues in 3GPP to identify future traffic challenges and develop LTE/LTE-A. LTE-MTC and NB-LTE-MTC are being developed to serve M2M and congestion control for M2M has been proposed in LTE.

The physical layer of LTE is based on Orthogonal Frequency Division Multiplex (OFDM). OFDM were considered for 3G systems, but was determined too immature, however OFDM has since then matured and is widely deployed in for example 802.11 (Wi-Fi) and Digital Video/Audio Broadcast (DVB/DAB). In addition to OFDM, multiple antenna techniques such as multiple-input-multiple-output (MIMO) has been emploeyed. MIMO may be used to increase the channel capacity by spatial multiplexing or enhance the signal robustness.

The scope of LTE features that is covered in this section is limited to PHY resource grid and access technologies for uplink and downlink in FDD mode.

3.1.1 Multiple access technologies

OFDM divides a wide band spectrum into several narrow-band sub-carriers. The sub-carriers are mutually orthogonal, which mitigates inter symbol interference (ISI). The bandwidth of each sub-carrier is smaller than the radio channel coherence frequency, which means there is no need for equalisers. The information to be transmitted is parallelized over the sub-carriers by Inverse Fourier Transforming (IFFT) modulated data symbols. The result is an OFDM symbol, which is transmitted over the radio interface, and can be interpreted in the receiver by applying the inverse operation, an FFT.

Mobile channels are time-dispersive so multiple replicas due to multipath will occur. Time dispersion is equivalent to frequency selectivity. Frequency selectivity may result in a loss of orthogonality between the sub-carriers. A guard period, or cyclic prefix (CP), T_G is added to the front of the OFDM symbol to negate this effect. The CP is a replica of a fraction of the end of the OFDM symbol.

OFDMA allows for the allocation of the sub-carriers with favourable propagation conditions for each user within a system. OFDM is as noted also robust to multipath and has no need for intra-cell interference cancellation. A drawback of OFDM is, however, that it is sensitive to frequency offset which arises from electronic instability and Doppler spread due to mobility. The latter can be mitigated by addition of the CP. OFDM also has a high peak-to-average power ratio (PAPR). PAPR leads to adjacent channel interference. PAPR can be mitigated by applying amplifier techniques. Such methods may be applied at the base station, but is too costly for UEs. Therefore in the uplink single carrier FDMA (SC-FDMA) is applied. SC-FDMA is implemented using a DFT to multiplex data in specific frequency allocation blocks as allocated by the uplink scheduler.

SC-FDMA does not provide orthogonality between the carriers and thus there is a need for equalization at the base station. SC-FDMA on the other hand is not as sensitive as OFDMA with regards to frequency offset and Doppler spread.

3.1.2 Physical parameters

In this subsection the parameters of the physical layer in LTE [16] is described.

The base time unit in LTE (T_s = 1/30720000) is used to express all other values in the time domain. The radio frame length is 10 ms, equivalent to 307200·T_s. Each frame is divided into 10 subframes of length 1 ms or 30720·T_s. Each subframe consists of two slots of equal length 0.5 ms (15360·T_s). Each slot consists of seven or six OFDM symbols depending on whether an extended CP is used. The extended CP mode extends the CP of each OFDM symbol from 4.7 μs to 16.7 μs. The extended CP mode is applied in very large cells and for low data rate applications.

The sub-carrier spacing Δf is equal to 15 kHz. The sampling rate f_s is give by $f_s = \Delta f \cdot N$. N being the number of sub-carriers. The number of sub-carriers varies

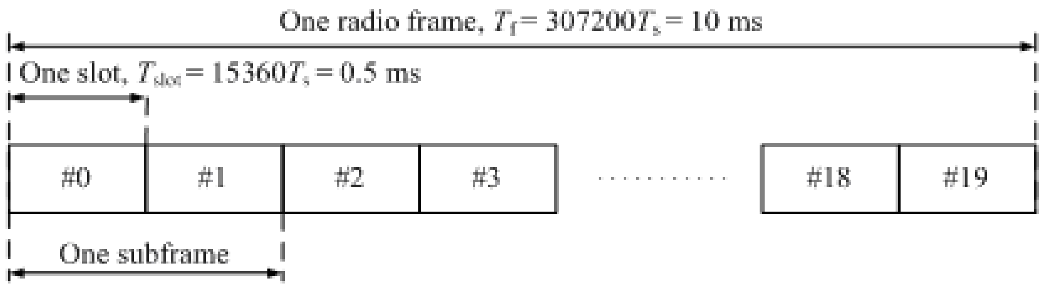

Figure 3.2: Frame structure type 1 (FFD) [16]

with the available channel bandwidth as seen in Table 3.1. To avoid causing interference some sub-carriers are used as guard bands in either side of the available bandwidth.

Transmissions are scheduled within resource blocks (RBs). An RB consists of 12 sub-carriers for the duration of one slot. A resource element is one sub-carrier for the duration of one OFDM symbol.

The resource structure is similar for the uplink, which is depicted in Figure 3.3. One resource element in the uplink is one sub-carrier (ie. 15 kHz of bandwidth) for one SC-FDMA data block length. A resource block consists of 12 REs for the duration of a slot. The minimum unit for scheduling is one RB hence the minimum bandwidth allocated for each UE is 180 kHz. The time domain parameters remain the same in the uplink as they were in the downlink. In the uplink UEs are assigned consecutive RBs while in the downlink the RBs are assigned in dispersive patterns.

3.1.3 Reference signals and synchronisation process

To allow for channel estimation in the downlink a few pilot symbols are transmitted. This takes up four REs per RB. In the uplink a reference symbol is sent as the fourth or third SC-FDMA symbol in each slot depending on whether normal or extended CP is being used. Another reference signal is the Sounding Reference Signal (SRS), which is transmitted over a wide bandwidth in the last SC-FDMA symbol in a subframe. The SRS allows the base station to measure channel conditions for each UE and provide channel dependent scheduling in the uplink. The SRS is highly configurable in terms of rate and may even not be configured at all.

Two synchronization signals are transmitted in the downlink to allow for UEs to synchronize sampling clock, carrier frequency and symbol offset. The synchronisation signals are called Primary Synchronization Sequence (PSS) and Secondary Synchronization Sequence (SSS). The PSS and SSS are transmitted in the last and second to last OFDM symbol of every 1st and 11th slot in each 10 ms frame, respectively. The PSS and SSS are placed in the central six RBs irrespective of the channel bandwidth such that UEs may synchronize to the network with no a priori knowl-

Table 3.1: LTE downlink physical parameters

Channel Bandwidth (MHz)	1.25	2.5	5	10	15	20
Frame Duration (ms)	10					
Subframe Duration (ms)	1					
Sub-carrier Spacing (kHz)	15					
Sampling Frequency (MHz)	1.92	3.84	7.68	15.36	23.04	30.72
FFT Size	128	256	512	1024	1536	2048
Occupied Sub-carriers	76	151	301	601	901	1201
Guard Sub-carriers	52	105	211	423	635	847
Number of Resource Blocks	6	12	25	50	75	100
Occupied Channel Bandwidth (MHz)	1.140	2.265	4.515	9.015	13.515	18.015
DL Bandwidth Efficiency	77.1%	90%	90%	90%	90%	90%
OFDM Symbols/Subframe	7/6 (short/long CP)					
CP Length (Normal CP) (μs)	5.2 (first symbol) / 4.69 (six following symbols)					
CP Length (Extended CP) (μs)	16.67					

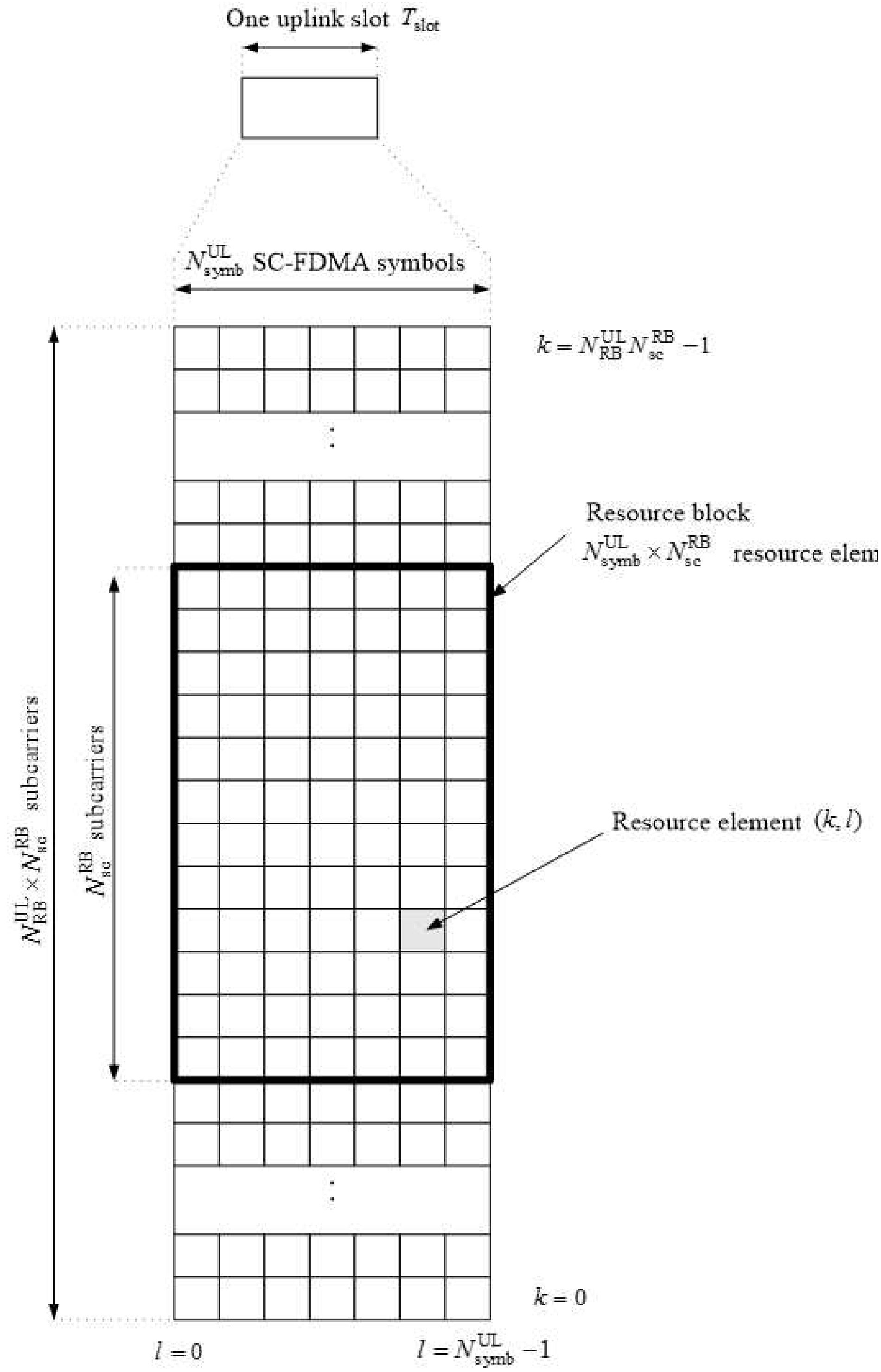

Figure 3.3: Uplink resource grid [16]

edge of the system bandwidth. PSS and SSS takes up 14 REs per RB every tenth slot.

3.1.4 Radio protocol architecture

In this subsection the radio protocol architecture for LTE is discussed. This includes a description of the protocol stack and the transport channels, logical channels and radio bearers defined by 3GPP [16, 15]. Many entities within the protocol are common to the user plane (U-plane) and the control plane (C-plane).

The LTE RAN provides Radio Bearers (atleast one) to which IP packets may be mapped according to their QoS requirements. The LTE protocol structure for uplink transmission is similar to the downlink transmission protocol structure with minor differences.

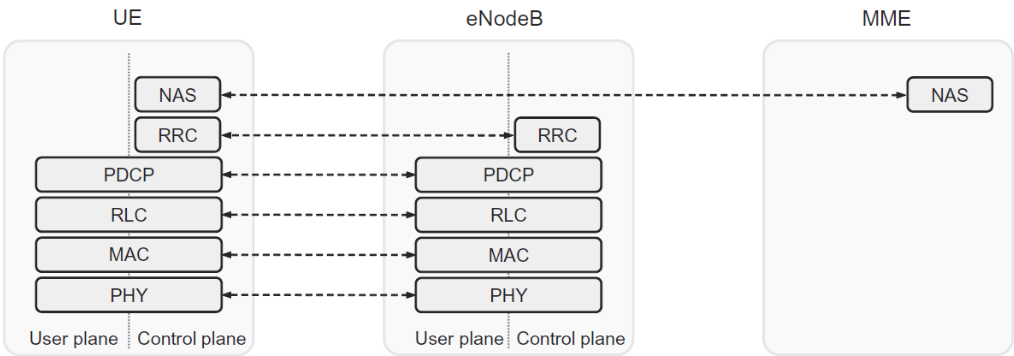

Figure 3.4: LTE protocol architecture [15]

In Figure 3.4 the overall protocol stack and its entities are depicted. In the U-plane the protocol entities and their responsibilities are:

- Packet Data Convergence Protocol (PDCP): IP header compression, ciphering, control plane, integrity protection and in-sequence delivery and duplicate removal.
- Radio-Link Control (RLC): Segmentation and concatenation, retransmissions, duplicate detection and in-sequence delivery. THE RLC layer provides Radio Bearers to the PDCP layer. One RLC entity is allocated for each radio bearer configured for a terminal.
- Medium Access Control (MAC): multiplexing of logical channels, HARQ and uplink/downlink scheduling. The scheduler for both uplink and downlink is located in the enodeB. The MAC layer provides logical channels to the RLC layer.

- Physical Layer (PHY): coding, modulation and MIMO. The PHY layer provides transport channels to the MAC layer.

The MAC layer multiplexes from the transport channels to the logical channels. The downlink channel mapping can be found in Figure 3.5.

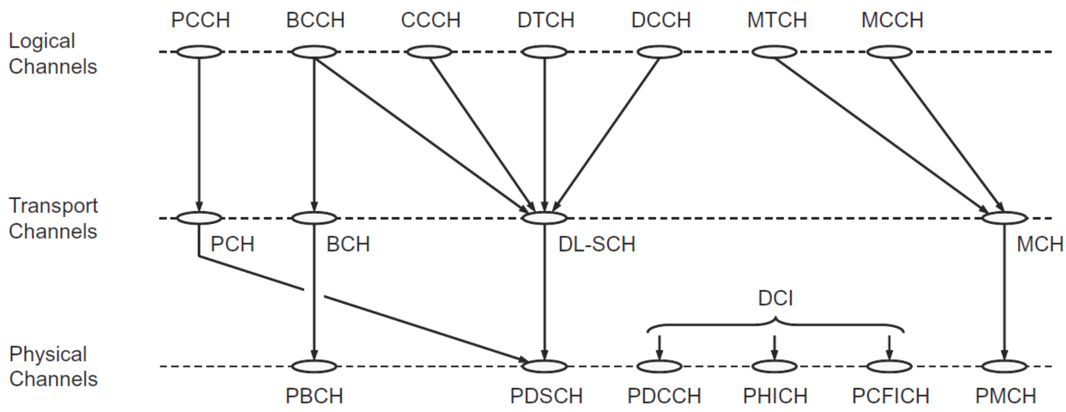

Figure 3.5: LTE downlink channel mapping [15]

Each channel provides different features for the layer above. The top layer channels provide abstractions from lower tier channels. The transport channels are of particular interest as random access and scheduling is handled in at this tier. In the downlink the transport channels and their respective services are:

- The Broadcast Channel (BCH): Used for transmission of system information.
- The paging channel (PCH): Used for paging in order to support discontinuous reception (DRX).
- The Downlink Shared Channel (DL-SCH): The channel carrying data in the downlink. This channel supports rate-adaptation techniques. harq, drx and spatial multiplexing.
- The Multicast Channel (MCH): Used for Multimedia Broadcast Multicast Services (MBMS).

In the uplink the transport channels are the Uplink Shared Channel (UL-SCH) and the Random Access Channel (RACH). The Uplink Shared Channel is the channel carrying uplink data while RACH is used for random access. Before attempting random access a LTE UE must first perform a cell search and synchronization and receive the cell system information. Cell searching and synchronisation to neighbouring cells in order to estimate the quality of neighbouring cells to handle hangovers must be done continuously after the random access procedure succeeds.

3.1.5 Transmission sequence and random access procedure

The initial transmission process involves performing RA and setting up a RRC connection.

1. Preample
2. Random Access Response
3. RRC Connection Request
4. RRC Connection Setup
5. RRC Connection Setup Complete
6. Security Mode Command
7. Security Mode Complete
8. RRC Connection Reconfiguration
9. RRC Connection Reconfiguration Complete
10. Payload transmission

The random access (RA) procedure in LTE is a four-step procedure. It is sued to move UEs from the RRC_IDLE state to the RRC_CONNECTED state. It is also used to re-establish radio connectivity upon radio-link failure, for handovers, to establish uplink synchronization and for dynamic scheduling-requests of resources if no resources have been dedicated for scheduling-requests.

1. RA preamble: The transmission of a preamble in the RACH channel. This allows for estimation of the UE timing in the enodeB and lets the UE pend the enodeB for resource scheduling.
2. RA response: The enodeB responds in the DL-SCH with a timing offset and an indication of the UL-SCH resources provided the RRC uplink signalling in step three of the RA procedure.
3. Terminal Identification: Transmission of UE identification in the allocated resources in UL-SCH.
4. Contention Resolution: RRC downlink response in DL-SCh, which is used to resolve contention issues. For example, if two users were to use the same preamble at the same time, they would both respond with message three and at the enodeB either both messages would fail, or one would be sufficiently strong for capture effect to take place. In either case, this message lets the UEs know who, if any, were successive in the RA.

After establishing a RRC connection the UE remains in RRC_CONNECTED state until a timer expires and the UE switches to RRC_IDLE state. In the connected state the UE may transmit without going through the initial initial transmission sequence.

3.1.6 LTE-MTC and NB-LTE-MTC

LTE-MTC (LTE-M) is part of release 12 and 13 and is still being developed. In LTE-M the channel is made up of a 1.4 mHz block divided into six resource blocks. An extended version of discontinuous repetition cycle (DRX) has been defined for LTE-M in order to allow power saving at UEs. DRX lets UEs sleep when they do not need to listen to the downlink. The power savings along with the reduced antenna complexity as a result of the reduced bandwidth makes LTE-M useful for M2M communications. LTE-M works within the regular LTE networks and architecture.

NB-LTE-M is another LTE based protocol, which is proposed to refarm GSM spectrum providing a single 200 kHz RB.

3.2 Simulator

This section provides insight into the features of a Matlab® based LTE/LTE-A simulator. The simulator is based on a four step simulation Procedure. The simulator provides a tool to evaluate the quality of service for a varying number of devices considering different traffic models for fractions of the device population.

1. Configuration
2. Traffic Generation
3. Protocol Simulation
4. Post Processing

Figure 3.6: Overall Simulation Model

3.2.1 Traffic Generation

Arrivals and associated payload sizes are generated based on the traffic model developed in Section 2.1.3. Coordinates, arrival times and the associated payloads are saved for each UE. A parameter is set for all UEs with traffic within the simulated period to indicate the first RA opportunity.

3.2.2 Protocol Simulation

Post generation of traffic for all UEs in the cell the generated UE struct is passed to the LTE simulator. The LTE simulator processes sequentially through the subframes within the simulation time with a resolution of 1 ms. A loop processes each subframe in which events take place. The logic of the simulator within the loop is depicted in Figure 3.7.

For each subframe it is checked whether any UEs wishes to transmit. Only UEs who are not transmitting may initiate a new transmission. A transmission in this context is a sequence of messages, which are exchanged over the air until the transmission is deemed to be a failure or the data message has been transmitted as the last message in the sequence. A UE can either be in a connected or idle state. In the idle state, which all UEs start in at the beginning of the simulation, a UE has

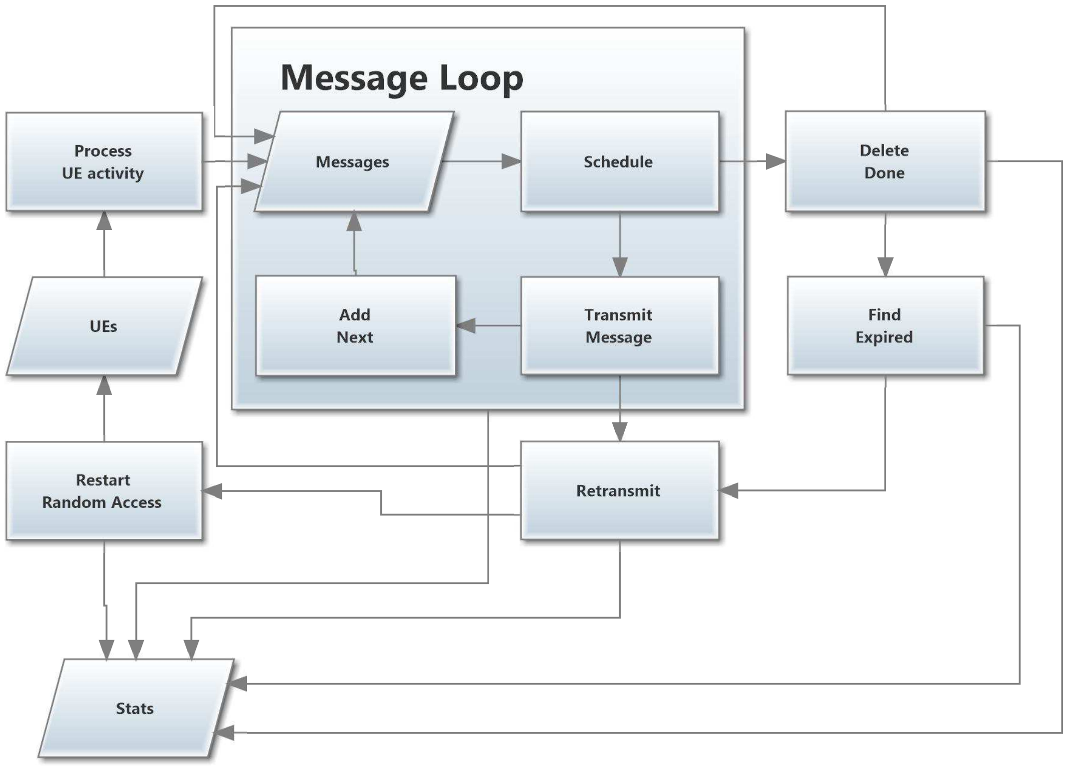

Figure 3.7: Simulation logic of LTE/LTE-A per subframe

to perform random access and establish a RRC connection before transmitting the data message. In the connected state a UE transmits just the data message. The state of a UE is changed from connected to idle based on inactivity seen from the base station for a configurable period.

Having added new messages to a FIFO message queue the simulation proceeds by working through the message queue starting with the oldest message. Each message passes through a scheduler, which finds whether enough resources are available to transmit the message in the PUSCH or PDSCH and whether enough control elements are available for signalling in the PDCCH. A transmission subroutine selects the modulation to be used for the transmission and calculates the BEP based on a link budget that includes path loss, shadowing and multipath and assumes a coherence time of 1 ms. With the modulation and BEP set for successfully scheduled messages they are passed to "Add Next", which evaluates whether the transmission has failed and should be passed to a retransmission function or, if successful, the next message in the transmission sequence should be placed in the message queue.

After all messages have been processed, the finished messages are removed from the message queue. As the message queue grows larger compared to the available resources the time before a message is served grows. This means that some message will experience their expiration timers to kick in. Such messages are found at this stage and passed to the retransmission function before being removed from the message queue.

The retransmission function looks up for each message passed to it, how many transmission trials it has undergone. If the number is at the limit L. The message is instead passed to a function to restart the random access procedure. If the number of trials is below L, a copy of the messages is placed in the back of the message queue.

The restart random access procedure sets the "next RA" of the corresponding UE to be at the next random access opportunity if the transmission RA attempts are under the limit M. Otherwise the transmission is reported to be a failure, it is dropped and the "next RA" of the UE is set for the next transmission of the UE, given that more transmissions were generated for the UE.

Success is reported upon the successful transmission of a data message.

Random Access

A "preamble" is transmitted when a UE has a transmission in a given subframe and the UE is not RRC connected.

The preamble has priorly been selected at random from the available preambles during the traffic generation. A random access response (RAR) message is transmitted by the base-station to signal detected preambles and scheduling grants. The terminal identification message is transmitted as a response by the UEs that transmitted the detected preambles. At this point collisions may occur if more than a single UE is transmitting a given preamble. Capture effect is not modelled. Collisions are not detected by the UEs, but since the BS is unable to respond to the terminal identification message the UE timers expire at which point random access is reinitialized.

Scheduling

The path-loss is calculated using Friis' path-loss equation. Based on a LTE carrier. The path-loss variance over different carriers in uplink and downlink is assumed negligible. Shadowing and fast-fading are selected at random from log-normal and Rayleigh distributions, respectively. Based on these parameters and the transmission power a link budget is established.

For data messages the modulation is selected to achieve the highest capacity possible while maintaining the bit error probability below or at target. QPSK is sued per default for any other messages and in this case the bit error probability is calculated.

The payload of data messages are bundled together before scheduling given that a UE has generated another payload to transmit before a transmission of the previous payload has been transmitted. Up to B transmissions may be bundled together in this manner. The amount of RBs needed for transmission of the message is calculated and fragmentation is applied, such that the message may be sent as fragments over several subframes. It is checked whether enough CCEs are in the PDCCH for DL allocations and UL grants.

The messsage is scheduled for transmission if both RBs in the UL/DL and CCEs in the PDCCH are available.

Adding Next Message

Scheduled messages are processed by this function. Each message is processed on it's own. Collisions are evaluated for Random Access Response messages. Preamble transmissions are received without error. Two or more transmissions of the same preamble results in a collision. The next message in the transmission sequence (MSG3) is added to the message queue regardless of collisions. Collisions are resolved upon the transmission of the MSG3.

On the transmission of any other message RAR it is evaluated whether the transmission has failed or not based on the error probability given by the AMC function. The payload of fragmented messages is updated given successful transmission.

RRC Connection

UEs are flagged as RRC_CONNECTED after a successful transmission of a data message and a RRC timer is set. The RRC connection is lost once the RRC timer expires.

The simulator has been optimized to jump to subframes with events. That is, if no message is in queue, the next subframe of interest is the time of the next transmission attempt. Any UE whose RRC connection expire is flagged as being in RRC_IDLE state and the next transmission attempt is set to the first random access opportunity after the time of the transmission attempt. If messages are in-queue the RRC expiration is handled at the end of each subframe.

The transmission sequence for an RRC_CONNECTED UE is reduced to the transmission of a data message.

Completed & Expired Messages

Messages which were scheduled are removed from the message queue to avoid duplicates. Messages whose timers expire are passed to a retransmission function. In both cases the statistics of said message are saved.

3.2.3 Simulation parameters

The simulation parameters are listed in Table 3.2.

Table 3.2: Simulation parameters

Parameter	Description	Value
Simulation length	Simulated period in seconds	50
Coding rate	Coding rate for the transport block	1/3
L	Maximum transmission trials in a sequence before attempting to reestablish connection starting with RA	4
M	Maximum number of RA attempts before dropping transmission	10
B	Maximum number of packets that may be bundled together	10
RAOs	Subframes in which preambles may be transmitted	1 in 10
BEP target	Target BEP for AMC	$5 \cdot 10^{-5}$

3.3 Results

In this section the results of the simulations are presented for the three traffic scenarios. The outage, mean latency, collision probability and probability of transmission error and error due to starvation is listed for each simulation in Table 3.3.

Table 3.3: Outage, mean latency, collision probability and probability of transmission error and error due to starvation.

Scenario	Outage	Latency [ms]	$P_{\text{Collision}}$	P_{TXerr}	P_{Starve}
Periodic	0	57.96	0.001	0.083	0.0294
Exception	0.191	439.4	0.305	0.078	0.15
Both	0.18	401.8	0.2924	0.079	0.14

The latency distributions for the three simulated scenarios are plotted in Figure 3.8 through Figure 3.13.

3.4 Discussion

LTE-M is seen to accommodate the periodic reporting with very low latency, but in the case of exception reports the network becomes congested due to the temporary very high arrival rates. More collisions occur and more messages transmissions are

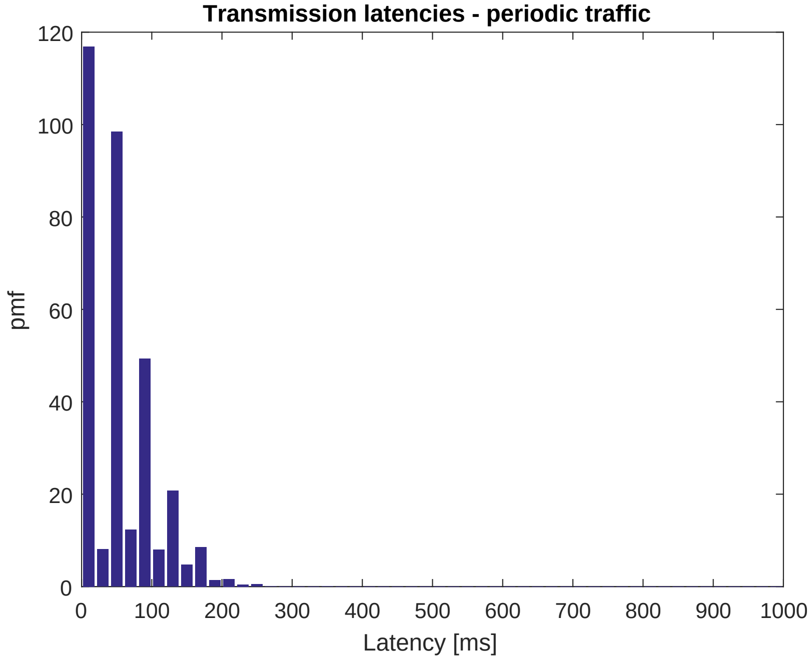

Figure 3.8: Histogram of transmission latencies for the regular reporting traffic

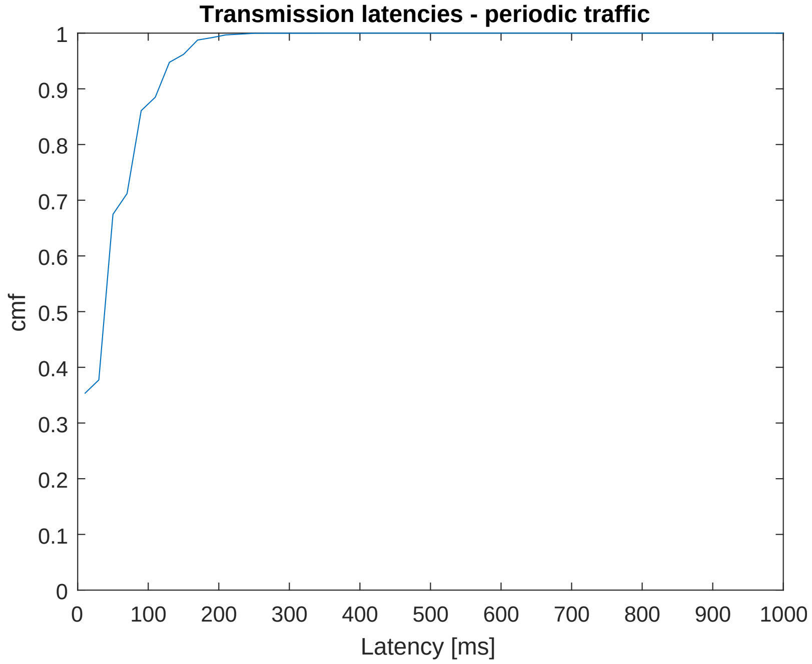

Figure 3.9: CMF of transmission latencies for the regular reporting traffic

starved of resources. In the case of exception traffic, messages are starved 75.4%

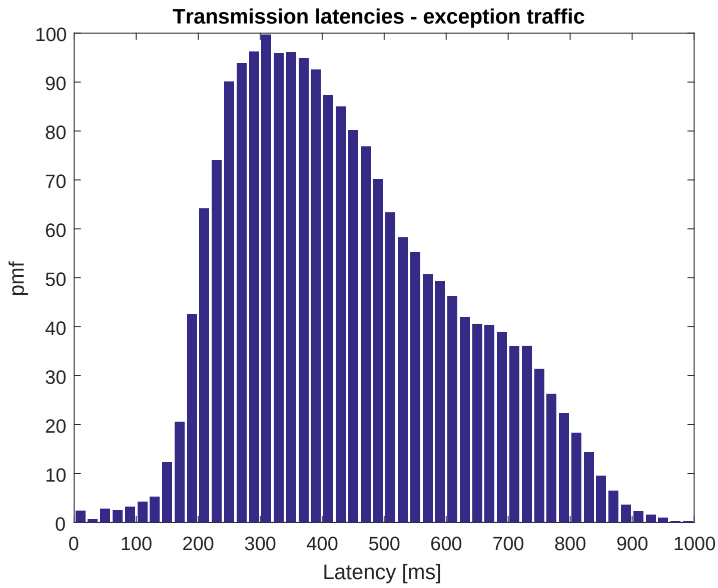

Figure 3.10: Histogram of transmission latencies for the regular reporting traffic

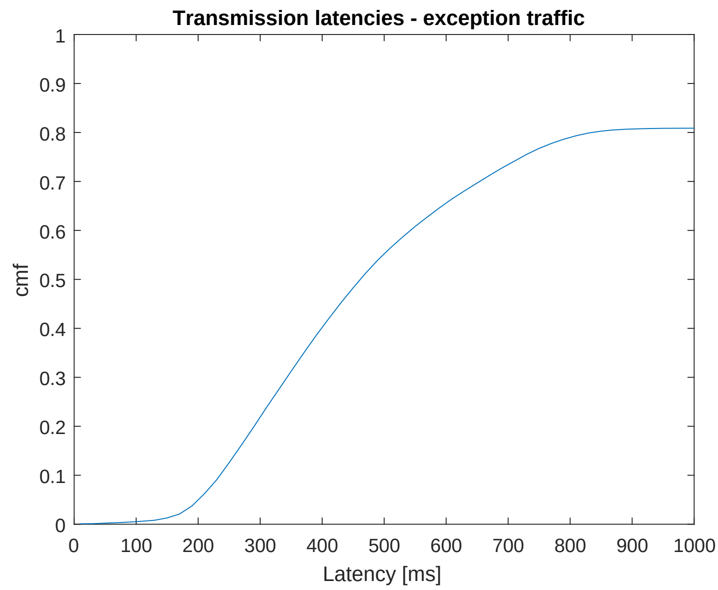

Figure 3.11: CMF of transmission latencies for the regular reporting traffic

of the time due to a lack of CCEs and 24.6% of the time due to a lack of RBs to transmit in. This ratio is a result which emphasizes the importance of signalling overhead in massive M2M.

The latency for periodic traffic was found to have a low mean and a low diver-

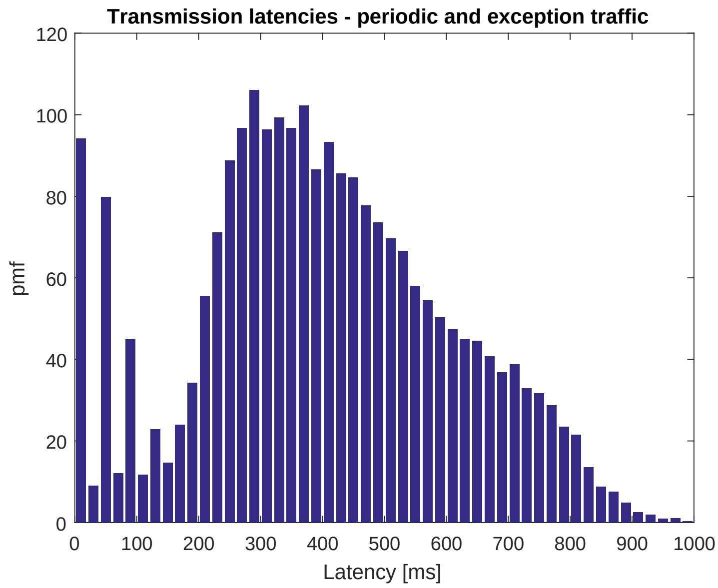

Figure 3.12: Histogram of transmission latencies for the regular reporting traffic

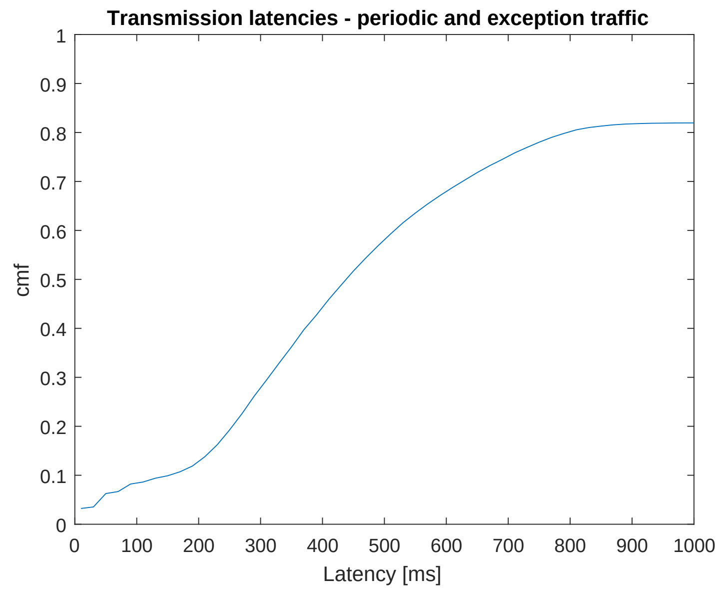

Figure 3.13: CMF of transmission latencies for the regular reporting traffic

sity due to low congestion. Contrary the diversity for exception reports was found to be large due to the congestion introduced in the network and the mean latency was considerably higher than for periodic traffic. Considering both traffic types we see that many packets are received while the network is congested due to the exception reports while some packets are received once the congestion has been resolved and are distributed as in the case of purely periodic reports.

Chapter 4

Long Range Wide Area Network

A LoRaWAN is a long range star topology LPWAN. In this chapter the performance of LoRaWAN is evaluated through a simulator, which is shown to fit to analytical results. LoRaWAN defines three different classes of nodes: A, B and C. Class A is the class with the minimal power consumption. Class A devices have bi-directional communication with a downlink receive window that follows uplink transmission. The assumed traffic model for massive low-complexity sensor networks uplink initiated traffic fits well with class A behaviour. Henceforth all LoRa devices are considered class A.

4.1 LoRaWAN

LoRaWAN is a MAC protocol based on the Long Range (LoRa) modulation as the PHY layer.

4.1.1 LoRa

LoRa is a proprietary spread spectrum modulation. LoRa is a derivative of Chirp Spread Spectrum (CSS) modulation. In LoRa a spectrum is spread by generating a chirp signal. This chirp signal eliminates frequency and timing offsets between transmitter and receiver. It is resistant to the Doppler effect. The chirp also offers resistance to multipath fading. It is a constant envelope modulation, which allows for cheap power efficient transceivers.

The data signal is chipped at a higher data rate and modulated onto the chirp signal. A high bandwidth-time product results in high robustness to interference and LoRa has high co- and adjacent channel rejection. The bit rate, chip rate and symbol rate are dictated by the spreading factor (SF). The symbol rate is given by (4.1). In one symbol period a chirp covers the entire bandwidth (BW).

$$R_S = \frac{1}{T_S} = \frac{BW}{2^{SF}} \tag{4.1}$$

SF is the number of bits transmitted per symbol, so the bit rate may be found as (4.2).

$$R_b(\mathrm{SF}, \mathrm{CR}) = SF \cdot \frac{BW}{2^{SF}} \tag{4.2}$$

The spreading factors employed in LoRa are orthogonal. The coding rate (CR), the SF and the BW ultimately decide the bit rates, which are listed in Table 4.1 for the defined SFs.

4.1.2 LoRaWAN

The LoRaWAN protocol is a MAC layer protocol. A gateway serves LoRa devices in a star topology. The gateway relays the messages to a central server. LoRaWAN implements an adaptive data rate (ADR) scheme, which can be used to maximize robustness, energy efficiency and capacity throughout the cell.

Uplink messages are transmitted as soon as it is possible for a LoRa device to do so while complying to local duty cycling regulations for the sub-band used. Downlink messages may only be received in a receive window. A receive window open a fixed amount of time after a uplink transmission has ended with a 20 ms margin of error. The minimum delay after an uplink transmission before a receive window opens is 1 second. A second receive window opens after a larger delay. The delay and data rate for each receive window can be customized. An acknowledgement retransmission procedure is defined, in which acknowledgements are send in the receive windows and retransmission occurs if no acknowledgement is received.

LoRaWAN also defines an initial procedure for securely joining a LoRaWAN. In the following a cell which has already been initialized is considered.

4.2 Analytical model

In this section a LoRaWAN scenario is defined and analytical model is presented. The shorthand LoRa will be used interchangeably with LoRaWAN in the following sections. The scenario consists of a single cell with LoRa devices. The devices have joined the network and been configured. It is considered that spreading factors 7 to 12 are available (no ADR) at all devices and that 16 channels of 125 kHz are allocated for LoRa.

Figure 4.1 shows a grid of the channels within a LoRa cell. A given SF in a given channel makes up a resource block (RB). The number of transmitting devices are spread uniformly over the available channels. Consider a single channel in which N devices are transmitting.

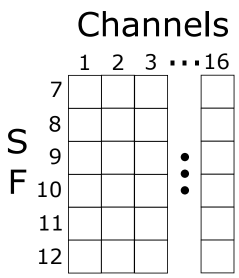

[h]

Figure 4.1: LoRa grid

The bit rate of a transmission in a RB is determined by the spreading factor and the CR within that RB. The coding rate is selected from 1 to 4.

$$R_b(\mathrm{SF}, \mathrm{CR}) = SF \cdot \frac{RC}{\frac{2^{SF}}{BW}} \tag{4.3}$$

where we define rate coding (RC) as

$$RC = \frac{4}{4 + CR} \tag{4.4}$$

The possible bit-rates are listed in table 4.1.

Table 4.1: Bit rates in LoRa

CR|SF	12	11	10	9	8	7
1	293	537	977	1758	3125	5469
2	244	448	814	1465	2604	4557
3	209	384	698	1256	2232	3906
4	183	336	610	1099	1953	3418

4.2.1 Latency

The transmission latency considering a 1-shot transmission of a device, which does not experience queueing delay due to duty-cycling, can be calculated from the rates given in table 4.1 by (4.3) and the transmission payload size. The assumption that no duty-cycling delay is experienced holds for very low-rate traffic such as the MAR periodic, but also for the MAR exception traffic since only a single report is transmitted per device. A minimum LoRa header size of 12 bytes is considered.

$$\tau(\mathrm{SF}, \mathrm{CR}, \mathrm{B}) = \frac{B}{R_b(\mathrm{SF}, \mathrm{CR})} \tag{4.5}$$

4.2.2 Capacity

The capacity of a LoRa channel is the maximum bit-rate that the channel is able to provide.

$$C_{ch,max} = \sum_{x=7}^{12} R_b(\mathrm{SF_x}, \mathrm{CR}) \tag{4.6}$$

Since the transmissions are spread uniformly over the channels we have that

$$C_{system,max} = C_{ch,max} \cdot n_{ch} \tag{4.7}$$

The capacity is only achievable when no devices transmit at the same SF in the same channel at the same time and the sensitivity requirement of the modulation is met.

4.2.3 Outage

A collision occurs when two or more devices transmit in the same RB at the same time. Upon a collision all transmissions within the RB is lost. Each SF can be considered a pure Aloha channel.

The SF is chosen uniformly from the available SFs, which are determined by the payload size. The maximum payload sizes are given in Table 4.2.

Table 4.2: Maximum payload sizes

SF	12	11	10	9	8	7
Max payload	51	51	51	115	222	222

The number of users in each pure aloha channel may then be found. The chance of collision in a pure Aloha channel is well known to be:

$$P_{Col} = 1 - P_{noTX} = 1 - e^{-2 \cdot L} \tag{4.8}$$

where the offered load L is defined as $L = N_{SF} \cdot \lambda \cdot \tau$ and τ is the transmission time given by the payload and transmission rate for the spreading factor.

4.2.4 Throughput

The throughput of each SF is given as

$$T = L \cdot e^{-2 \cdot L} \tag{4.9}$$

The average data rate is then given by

$$R_{SF} = L \cdot P_{noTX} \cdot R_b(\mathrm{SF_x}, \mathrm{CR}) \tag{4.10}$$

and given nCH channels the rate for the cell can be found as

$$R_{cell} = \sum_{x=7}^{12} R_{SFx} \cdot nCH \tag{4.11}$$

4.3 Simulation

Figure 4.2 depicts the structure of a simple LoRa simulator. The simulator uses the same traffic generator and UE structs as the LTE simulator. Any transmissions are transmitted in a random channel using a random SF with a latency computed using (4.2.1). Collision are flagged in the post-processing in which outage, latency and throughput are found.

Figure 4.2: LoRa simulation

4.4 Results

In this section the simulation is shown to fit to the analytical model for Poisson distributed traffic generation. Simulated results for each of defined traffic scenarios are then displayed.

Figure 4.3 depicts the capacity of LoRa and simulated and analytical throughput. The capacity is scaled to the maximum efficiency for each SF. The rate is found with equal arrival rates for each SF. The efficiency differs for each SF for a given arrival rate as the offered load depends on the transmission time, which results in a throughput that is below the capacity of the aloha LoRa channel.

The collision probability also varies over the SFs given an arrival rate due to the different transmission times. This means that all SFs do not offer a "fair" success rate compared to each other. In practise the selection of SF should not be based on a uniform distribution, but rather a distribution scaled to the relative transmission times. The distribution should be scewed a bit to keep the higher SFs uncluttered to allow for long range transmissions and transmissions for devices with poor channel conditions.

The simulated and modelled collision probability for each SF is depicted in Figure 4.5 for the MAR periodic reports defined in Chapter 2.

The outage, mean latency and bit rate for LoRa with respect to the three defined traffic scenarios may be found in Table 4.3.

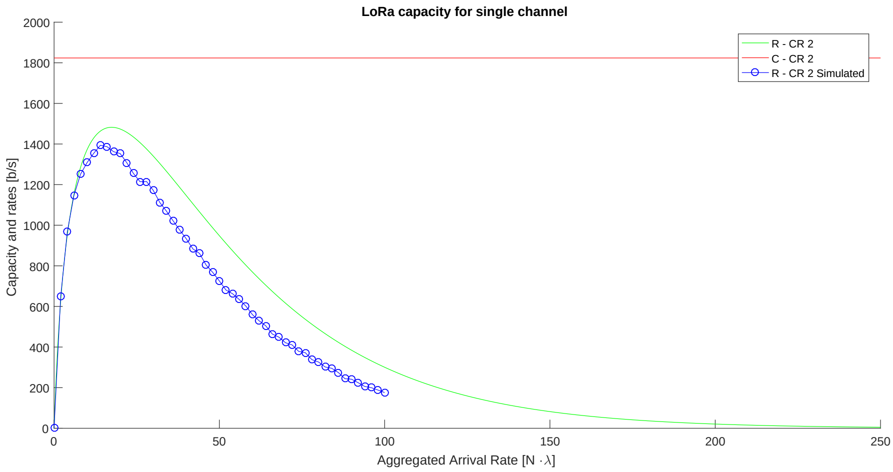

Figure 4.3: LoRa system capacity and bit rates

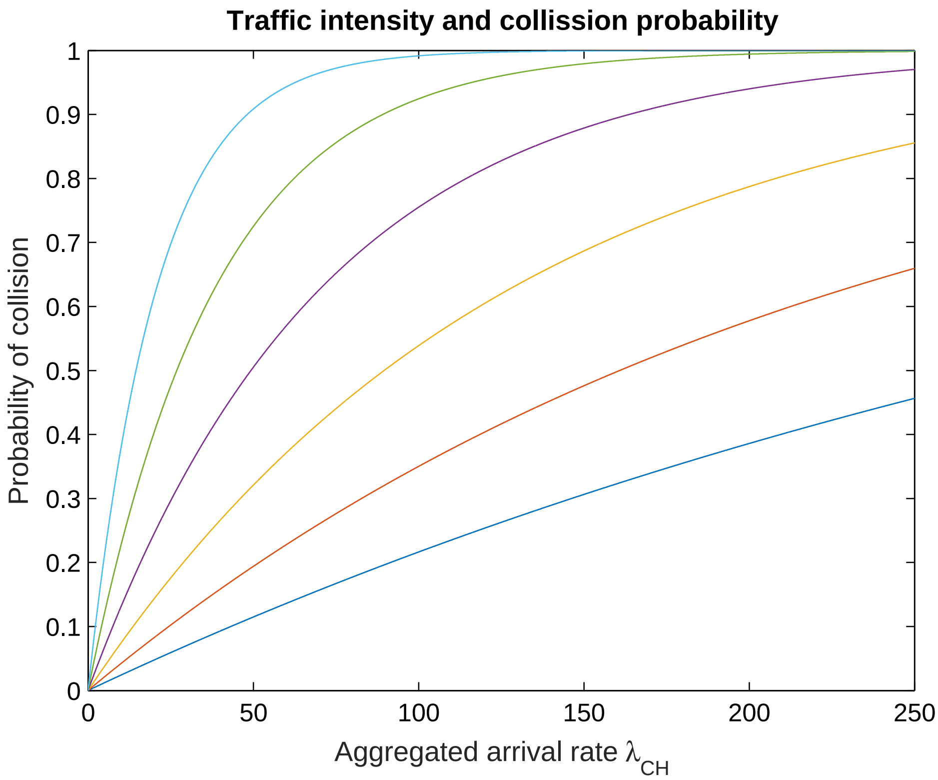

Figure 4.4: LoRa collision probability for each spreading factor. λ_{CH} is the aggregated arrival rate per channel.

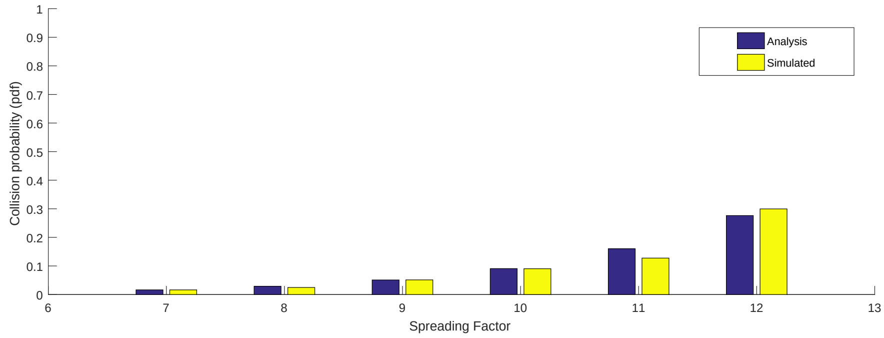

Figure 4.5: LoRa pois

Table 4.3: Outage, mean latency and bit rates for LoRa with respect to the defined traffic scenarios

Scenario	Outage	Delay [ms]	Bit rate [b/s]
Pois (analytical)	0.104	740,8	3309,5
Pois (simulated)	0,096	730	2989,9
Beta	0,733	143,5	1118,4
Both	0,678	216	1517,4

4.5 Discussion

The presented 1-shot model and simulation found LoRa to have a 10% outage for the periodic reporting traffic. The model and simulation do not take duty cycling into account, which would cap the arrival rate for each device at a service rate and impact the latency once the traffic generation rate increases beyond the service rate.

In the 1-shot form, however, LoRa was shown to not completely accommodate periodic reporting, but may be used for offloading some of the traffic or as a redundant networking interface. The outage may be lowered in scenarios with a low system load by transmitting the same packet multiple times for redundancy. The uniform distributions of spreading factors also have a negative impact on the outage, which could potentially be bettered with proper ADC.

In the case of Exception traffic the Beta distributed reports result in a very high probability of collision due to the aloha-type protocol for many reports and a low collision probability for fewer reports. This conclusion may be drawn from figure 4.4 observing that the temporal distribution of exception reports can be modelled as a Beta modulated Poisson process.

Chapter 5

Mixed architectures

In this chapter the use of dual interfaces, specifically LoRa and LTE-M, is investigated.

5.1 Scenarios

Devices throughout a cell may have either a LoRa interface, a LTE-M interface or both. The LoRa interface is the cheapest interface. LoRa can not provide the same QoS reassurances as LTE-M, but is sufficient for non-critical sensor measurement reporting. LTE-M on the other hand is more expensive, but provides QoS reassurances, which allow larger payload sizes, higher arrival rates and higher reliability for more critical M2M traffic. The two interfaces may also be combined for redundancy or to offload massive access from, for example, non-critical sensors in LTE-M through capillary networks. The transmission scenarios in such a cell are outlined in Figure 5.1.

5.1.1 Redundant interface

In this scenario very critical reports could be sent on two interfaces by the machine type device. The chance of outage would then be the chance that both interfaces fail to transmit successfully

$$P_O = P_{O,LTE} \cdot P_{O,LoRa} \tag{5.1}$$

The latency would be the minimum latency of a successful transmission to the end-point. The mean latency would then be given as (5.2).

$$L = \frac{P_{S,LoRa} \cdot P_{S,LTE} \cdot min(L_{LTE}, L_{LoRa}) + P_{S,LTE} \cdot P_{O,LoRa} \cdot L_{LTE} + P_{S,LoRa} \cdot P_{O,LTE} \cdot L_{LoRa}}{P_{S,LoRa} \cdot P_{S,LTE} + P_{S,LTE} \cdot P_{O,LoRa} + P_{S,LoRa} \cdot P_{O,LTE}} \tag{5.2}$$

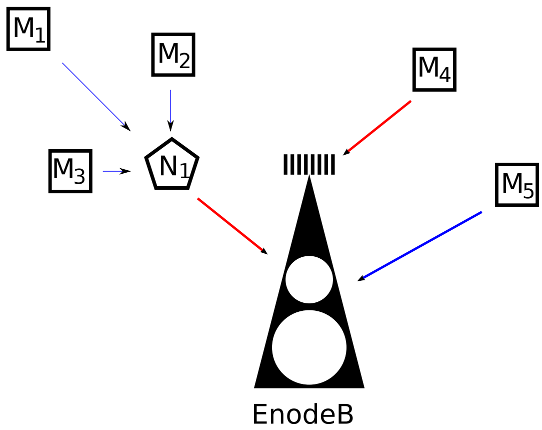

Figure 5.1: Capillary relaying and direct links within a cell. Machine type devices are denoted by M, Aggregators by N, LoRa connections are marked by blue and LTE connections are marked by red.

The mean capacity is given in an equivalent way

$$C = \frac{P_{S,LoRa} \cdot P_{S,LTE} \cdot max(C_{LTE}, C_{LoRa}) + P_{S,LTE} \cdot P_{O,LoRa} \cdot C_{LTE} + P_{S,LoRa} \cdot P_{O,LTE} \cdot C_{LoRa}}{P_{S,LoRa} \cdot P_{S,LTE} + P_{S,LTE} \cdot P_{O,LoRa} + P_{S,LoRa} \cdot P_{O,LTE}} \tag{5.3}$$

Redundant transmission make sense for critical transmissions especially when LTE-M becomes congested. In this scenario for real-time latency requirements, a higher SF should be used in LoRa to provide lower latency.

5.1.2 Capillary networks

Capillary networks may be used to offload massive access from LTE-M to the capillary network. This network has the added benefit of cheaper interfaces than LTE, for example LoRa, may be used in the capillary network. INstallation of a capillary architecture would only require deployment of the capillary gateways, assuming that the capillary network gate ways would relay transmissions to the BS by LTE.

While capillary networks insert another point of failure in the transmission line, they remove the need for massive random access from the cellular network which potentially increases the chance of successful transmission in the cellular network. Capillary networks also allow for aggregation of reports, which are non-critical, which also decrease the outage in the cellular network by decreasing signalling and increasing the efficiency.

The chance of a successful transmission through a capillary network is

$$P_S = P_{S,LTE}(\lambda_{LoRa}) \cdot P_{S,LoRa}(\lambda_T) \tag{5.4}$$

In (5.4) $P_{S,LTE}$ and $P_{S,LoRa}$ are written as functions to emphasize that $P_{S,LTE}$ is a function of the successful traffic rate of LoRa.

The latency is the sum of the latencies of the two transmissions, including relay processing.

$$L = L_{LoRa} + L_{LTE} \tag{5.5}$$

The capacity is given as

$$C = \frac{C_{LoRa} + C_{LTE}}{2} \tag{5.6}$$

5.2 Results

Simulated results for the two transmission scenarios are presented here.

5.2.1 Redundant Interface

The simulations of the LoRa and LTE interfaces have been carried out in earlier chapters and the results of using both interfaces for redundant transmissions are listed in Table 5.1. As expected for any interface with an outage probability lower than 1 having a redundant interface lowers the chance of being in outage. It is also observed that adding a LoRa interface for redundancy lowers the mean latency in the case of exception traffic. This is due to successful LoRa transmissions in this traffic scenario in the model examined in this work being primarily transmitted with low spreading factors.

Table 5.1: Redundant interface metrics calculated using simulation results

Scenario	Outage	LoRa outage	LTE outage	L [ms]	L_{LoRa} [ms]	L_{LTE} [ms]
Periodic	0	0,096	0	274.31	730	57.96
Exception	0.14	0.734	0.191	328.78	143.5	439.4
Both	0.122	0.678	0.18	324.36	216	401.8

5.2.2 Capillary network

A simulator for capillary networks has been made by combining the LoRa and LTE simulators. The overall flow of this simulator is to generate traffic, simulate LoRa and then simulate LTE given the successful LoRa transmissions as a traffic input. The simulated results can be found in Table 5.2. These results have been found without taking into account the capture effect and they show how the single LoRaWAN can not handle the same amount of traffic as the LTE cell and becomes the single point of outage.

Table 5.2: Capillary network simulation results - no capture effect

Scenario	Outage	LoRa outage	LTE outage	L [ms]	L_{LoRa} [ms]	L_{LTE} [ms]
Periodic	0.198	0.198	0	1540	1448.2	55.8
Exception	0.734	0.734	0	281.79	144.85	136.94
Both	0.693	0.693	0	567.98	450.84	117.14

5.2.3 N capillary networks and capture model

A capture effect model was introduced to the LoRa simulator to make a link-level simulator. The capture effect in LoRa is considered to take place when a signal is received at 1 dBm higher power and the stronger transmission started no more than 3 symbols after the weaker one. These parameters were found to yield a very high probability of successful transmission due to capture effect for the stronger transmission in [17]. Only path-loss is considered to have an impact on the received power and a path-loss exponent of 4 is considered.

The three traffic scenarios have been simulated with different numbers of capillary networks. The placements of the LoRa gateways have been found as the solutions to a circle packing problem. The outage for a varying number of capillary networks may be found in Figure 5.2. It is seen that the outage is lowered by adding more gateways. The outage for a single gateway is also lowered when considering the capture effect.

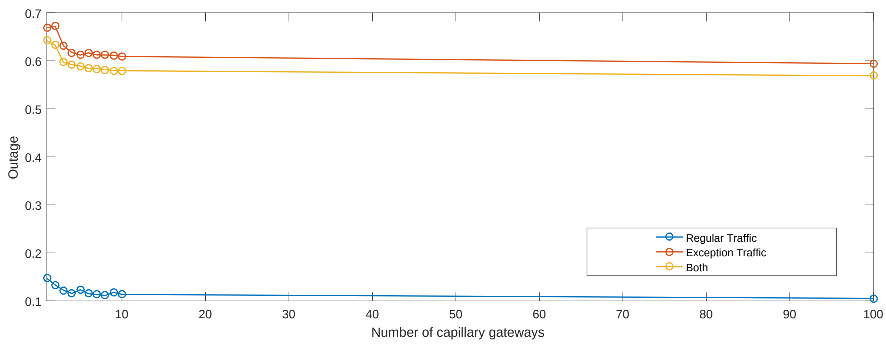

Figure 5.2: Outage in capillary network(s) for a varying number of LoRa gateways

The resulting QoS of having 4 capillary LoRa networks within one cell may be found in Table 5.3.

Table 5.3: Capillary network simulation results considering 4 LoRa gateways - capture effect

Scenario	Outage	LoRa outage	LTE outage	L [ms]	L_{LoRa} [ms]	L_{LTE} [ms]
Periodic	0.116	0.116	0	1623.8	1579.4	44.4
Exception	0.617	0.617	0	203.45	188.95	14.5
Both	0.592	0.592	0	471.1	454	17.1

Chapter 6

Conclusion

In this project a traffic model for low-rate massive M2M has been established in Chapter 2. The performance of LTE-M and LoRaWAN has been evaluated in Chapter 3 and Chapter 4, respectively. Dual interface scenarios have been investigated in chapter 5.

6.1 LTE-M

LTE-M was found to accommodate periodic reporting from 52200 low-rate IoT devices without outage and a mean latency below 60 ms. The outage was found to increase for exception reporting over 10 s with a 5% penetration to 19.1% and an increase in mean latency and latency diversity was observed. This result is expected as the temporal distribution of exception traffic is Beta distributed. Many transmissions will take place in the same period when the network is congested, less take place while the network is less congested and only a few transmission take place in the periods at the start and end of the temporal distribution period in which there is no congestion in the network. It was found that the chance of starvation of a message was increased to 15% for the exception traffic. The starvation factor due to lack of CCEs and RBs were found to be 3/4, and 1/4, respectively. Exception reports have a small 20 bytes payload. A RA message sequence has to be exchanged for each report transmission, which means there is a considerable signalling overhead which will take up network resources. Although the payload size is small it will take up an entire RB leading to inefficient channel use. The load on the control channel elements were in total, however, a bottleneck to the RBs.

LTE-M takes up 1.4 MHz and has the ability to be installed by a software update at a LTE BS, which makes LTE-M scalable and readily deployable.

6.2 LoRa

LoRa was found to have an outage of 10% and a mean latency of 740.8 ms under the load of periodic reporting traffic. Multiple transmissions per report was suggested as a way to decrease the outage in LoRa when the traffic load is low. Exception traffic prompted an outage of 73.3% in LoRa. This outage may be acceptable considering that the exception reports are likely triggered by a single event. A central server may likely deduce that an exception event has occurred for the devices in outage for the devices in outage, based on the successful transmissions. The mean latency and latency diversity of LoRa was shown to decrease with increasing traffic load.

6.3 LoRa as a redundant interface

LTE-M accommodates the periodic traffic without the need of an redundant interface. LoRa may, however, decrease the outage probability and mean latency when used as a redundant interface for exception events. The cost of two interfaces and the decrease in outage is a tradeoff, which makes this approach suitable for critical alarm reporting devices.

6.4 LoRa as capillary network

Capillary LoRa networks may offload massive access in LTE-M and reduce signalling in and more efficiently use RBs by aggregating reports in the LoRa gateways. Although capillary networks purely consisting of LoRa was shown to bottleneck LTE-M, this approach has promise to significantly lower the chance of collisions during RA in LTE and lower the chance of starvation. Also the cost of a LTE-M modem is moved away from the devices to the gateway instead.

6.5 Assesment of LTE-M and LoRa roles in cellular M2M

The four transmission strategies outlined through this report each have different advantages and disadvantages. The transmission scheme should be chosen on the device side based on a cost-QoS trade-off. The cheapest interface, LoRa, would be sufficient for low rate sensors in a low density environment. Deploying capillary LoRa networks results in a limited gain, enabling such an implementation to be sufficient in deployment scenarios with a slightly higher device density. LTE-M is attractive due to its high capacity, low outage and low mean latency. It is, however, the more costly approach. The modems are expected to be more expensive than LoRa modems and a portion of the LTE spectrum also has to be refarmed for LTE-

M. Redundant transmission is attractive due to the decrease in outage probability, however it is the most costly transmission strategy.

6.6 Perspective

As mentioned in Chapter 1 many protocols are competing on the IoT scene. This include SIGFOX, Weightless, 802.11ah, NB IOT, EC-GSM. The results obtained in this work enables comparison between LoRa and LTE-M and other protocols. A comparison between all protocols to evaluate the scenarios in which the specific protocol is advantageous would be very beneficial for device makers.

A Short range high capacity protocol could provide high data rates at energy efficient power levels with fewer inter-capillary collisions and potentially not bottleneck LTE-M. A dual interface modem allowing for transmissions with such a protocol in urban environments and LoRa, or another LPWAN protocol, could allow universal deployment of any low-rate device. This method does however require an investment in capillary gateways.

Bibliography

[1] A. Osseiran et al. "The Foundation of the Mobile and Wireless Communications System for 2020 and Beyond: Challenges, Enablers and Technology Solutions". In: (2013), pp. 1–5. ISSN: 1550-2252. DOI: 10.1109/VTCSpring.2013.6692781.

[2] AB Ericsson. "Interim Ericsson Mobility Report". In: (June 2014), p. 29.

[3] *Service requirements for Machine-Type Communications (MTC)*. TS 22.368. V13.1.0. 3GPP. Dec. 2014.

[4] *Study on RAN Improvements for Machine-type Communications*. TR 37.868. V11.0.0. 3GPP. Sept. 2011.

[5] G.C. Madueno, C. Stefanovic, and P. Popovski. "Reengineering GSM/GPRS towards a dedicated network for massive smart metering". In: *Smart Grid Communications (SmartGridComm), 2014 IEEE International Conference on*. 2014, pp. 338–343. DOI: 10.1109/SmartGridComm.2014.7007669.

[6] J.J. Nielsen et al. "What can wireless cellular technologies do about the upcoming smart metering traffic?" In: *Communications Magazine, IEEE* 53.9 (2015), pp. 41–47. ISSN: 0163-6804. DOI: 10.1109/MCOM.2015.7263371.

[7] J. J. Nielsen et al. "A Tractable Model of the LTE Access Reservation Procedure for Machine-Type Communications". In: *2015 IEEE Global Communications Conference (GLOBECOM)*. 2015, pp. 1–6. DOI: 10.1109/GLOCOM.2015.7417529.

[8] G. C. Madueño et al. "Assessment of LTE Wireless Access for Monitoring of Energy Distribution in the Smart Grid". In: *IEEE Journal on Selected Areas in Communications* 34.3 (2016), pp. 675–688. ISSN: 0733-8716. DOI: 10.1109/JSAC.2016.2525639.

[9] *Study on Machine-Type Communications (MTC) and other mobile data applications communications enhancements*. TR 23.887. V12.0.0. 3GPP. Dec. 2013.

[10] *System improvements for Machine-Type Communications (MTC)*. TR 23.888. V11.0.0. 3GPP. Sept. 2012.

[11] *Updated scenarios, requirements and KPIs for 5G mobile and wireless system with recommendations for future investigations*. ICT-317669-METIS/D1.5. V1. METIS. May 2015.

[12] *Cellular System Support for Ultra Low Complexity and Low Throughput Internet of Things*. TR 45.820. V2.1.0. 3GPP. Aug. 2015.

[13] G. Madueño, C. Stefanovic, and P. Popovski. "Reliable and Efficient Access for Alarm-initiated and Regular M2M Traffic in IEEE 802.11ah Systems". In: *IEEE Internet of Things Journal* PP.99 (2015), pp. 1–1. ISSN: 2327-4662. DOI: 10.1109/JIOT.2015.2496418.

[14] Magnus Olson et al. *EPC and 4g Packet Networks*. 2nd. Academic Press, 2014. ISBN: 978-0-12-394595-2.

[15] Erik Dahlman, Stefan Parkvall, and Johan Skold. *4G: LTE/LTE-Advanced for Mobile Broadband*. 2nd. Academic Press, 2014. ISBN: 012385489X, 9780123854896.

[16] *E-UTRA: Physical channels and modulation*. TR 36.211. V12.7.0. 3GPP. Sept. 2015.

[17] Martin Bor, John Vidler, and Utz Roedig. "LoRa for the Internet of Things". In: *Proceedings of the 2016 International Conference on Embedded Wireless Systems and Networks*. EWSN '16. Graz, Austria: Junction Publishing, 2016, pp. 361–366. ISBN: 978-0-9949886-0-7. URL: http://dl.acm.org/citation.cfm?id=2893711.2893802.